

Effects of Ce on damping capacity of AZ91D magnesium alloy^①

HUANG Zheng-hua(黄正华), GUO Xue-feng(郭学锋), ZHANG Zhong-ming(张忠明)

(School of Materials Science and Engineering, Xi'an University of Technology, Xi'an 710048, China)

Abstract: The microstructures and damping capacity of AZ91D cast alloys containing various Ce contents were investigated. Damping capacity (Q^{-1}) of the alloys was measured by cantilever beam technique, and the relationship between damping capacity and strain amplitude was investigated. The results show that Al_4Ce phase is formed in AZ91D alloy after adding a certain quantity of Ce contents, then as-cast microstructures of the alloys are refined. Meanwhile the damping capacity of the alloys is also improved. When the mass fraction of Ce is 0.7%, the most obvious refinement effect and the maximum damping capacity can be obtained. When the damping capacity (Q^{-1}) is 2.728×10^{-3} , 61% increment can be obtained compared with unmodified AZ91D alloy. The damping capacity of the alloys is relative to strain amplitude, and the damping behavior can be explained by the theory of Granato and Lüke.

Key words: damping capacity; damping mechanism; AZ91D alloy; Ce modification

CLC number: TG 146; TG 113

Document code: A

1 INTRODUCTION

The damping capacity is a measure of the energy dissipated during mechanical vibration in the materials or component. Metallic materials having high damping capacity become valuable in suppressing mechanical vibration and attenuating wave propagation for the control of noise and the stabilization of structures. Taking high damping metallic materials as structural parts could eliminate the need for special energy absorbers or dampers to attenuate the vibration and noise, in spite of most of the frequently used metals and alloys, which exhibit a relatively low damping capacity and are limited in their applications in dynamic structures. Therefore, material researchers have sought to improve the damping capacity of metals and alloys through the use of innovative material-processing techniques and alloying^[1]. Magnesium alloys as a whole have a high damping capacity among metallic structural materials and attractive mechanical properties, i.e. high specific strength and stiffness. Therefore, they are widely used in automotive, communicated, electronic and aerial industries^[2-4]. Although AZ91D alloy, being the most widely used die casting alloy, has been studied widely^[5, 6], the concern was focused on their mechanical and processing properties and the effects of trace elements on damping capacity were rarely studied yet^[7-9]. Some investigations

found that Ce-rich mischmetal had effective modification on grain refining and mechanical properties of AZ91D alloy at ambient and elevated temperatures^[10-13]. However, the effects of Ce content on damping capacity of AZ91D alloy remained unclear. Therefore, this paper is focused on the appropriate content of Ce with which appropriate damping capacity can be achieved. Meanwhile the damping mechanism of the alloys is also discussed.

2 EXPERIMENTAL

2.1 Materials and specimen preparation

The nominal chemical compositions of commercially used AZ91D alloy are shown in Table 1. Ce was added into the studied alloys in the form of Ce-rich mischmetal (50% Ce). The alloys were melted in a crucible resistance furnace. The Ce-rich mischmetal was added into the melt at 760 °C to prepare alloys that contained Ce of 0, 0.1%, 0.3%, 0.5%, 0.7% and 1.0%, respectively (in mass fraction). After adding the Ce-rich mischmetal, the melt was stirred for 8 - 10 min with a graphite rod and kept for 5 - 10 min for complete dissolution of the mischmetal. When the melt was cooled to 700 °C, the slag was skimmed off, then the melt was poured into a preheated permanent mold of 400 °C. During the melting and pouring processes, the melt was protected by $CO_2 + 0.3\% SF_6$ (volume fraction) mixture gas.

① **Foundation item:** Project(50271054) supported by the National Natural Science Foundation of China; project supported by the State Educational Ministry for Scientific Research Foundation for the Returned Overseas Chinese Scholars; project supported by the Open Foundation of State Key Laboratory of Solidification Processing

Received date: 2003 - 08 - 14; **Accepted date:** 2003 - 12 - 10

Correspondence: HUANG Zheng-hua; Tel: + 86-29-82312009; E-mail: huangzhenghua312@sina.com

The damping specimens were sectioned by electric spark erosion from the casting specimens. The dimensions of the damping specimens are $90\text{ mm} \times 5\text{ mm} \times 2\text{ mm}$ with a tolerance of $\pm 0.1\text{ mm}$ on each side. The surfacial roughness of each damping specimen is less than $1.6\text{ }\mu\text{m}$.

Table 1 Nominal chemical compositions of commercially used AZ91D alloy (mass fraction, %)

Al	Zn	Mn	Si	Fe
8.950	0.632	0.261	0.022	0.000 3
Cu	Ni	Be	Mg	
0.001 8	0.000 5	0.000 3	Bal.	

2.2 Damping capacity measurement

The measurement of damping capacity utilized is inverse quality factor (Q^{-1}) in this paper. Damping capacity of the alloys was measured by cantilever beam technique at ambient temperature. One end of the specimen was held in place, while the other end was pulled by various loadings for obtaining various strain amplitudes. The free end was allowed to vibrate when the loadings were wiped off instantly. A computer was used to record the history of amplitude vs time during free vibration of the specimen. Inverse quality factor (Q^{-1}) was obtained through a series of computations. During the test, the frequency is 177 Hz and the strain amplitude range is between 33×10^{-6} and 320×10^{-6} .

2.3 Microstructural characterization

The specimens were polished and etched with 4% HNO_3 in ethanol utilizing standard metallographic techniques. Microstructural observation was carried out on a Nikon Epiphot Optical Microscope. The phase compositions were analyzed by using the Rigaku D/max-3C X-ray Diffractometer, with $\text{CuK}\alpha$ radiation source and 0.02° step length. The scanning range was between 10° and 80° .

3 RESULTS AND DISCUSSION

3.1 Damping capacity

Fig. 1 shows the plot of damping capacity of AZ91D alloy vs Ce content at the strain amplitude of 9.3×10^{-5} . The experimental results reveal that the damping capacity is 1.699×10^{-3} for the unmodified AZ91D alloy, and increases with the increase of Ce content. The damping capacity reaches a maximum of $Q^{-1} = 2.728 \times 10^{-3}$ when the Ce content increases to 0.7%. The result shows that the damping capacity is increased by 61% compared with the unmodified AZ91D alloy. However, the damping capacity will

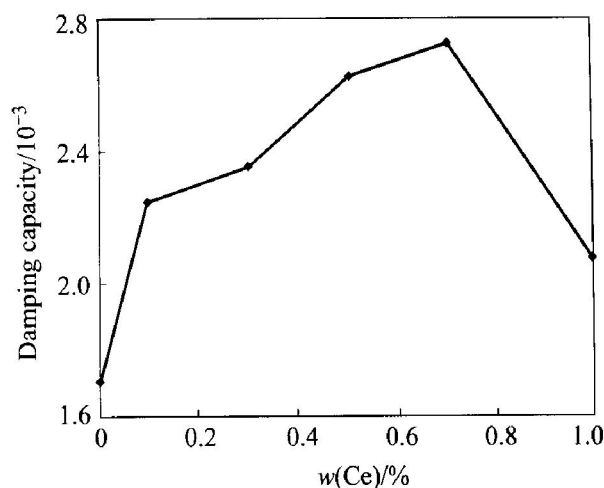


Fig. 1 Plot of damping capacity of AZ91D alloy vs Ce content

decrease when the Ce content is over 0.7%. Therefore, 0.7% Ce could be a reasonable content to improve the damping capacity of AZ91D alloy.

3.2 Microstructures

The variance of damping capacity of the alloys is related to the difference of their microstructures. Fig. 2 shows the microstructures of AZ91D alloys containing various Ce contents. The microstructure of as-cast AZ91D alloy is composed of $\alpha\text{-Mg}$ matrix and $\beta\text{-Mg}_{17}\text{Al}_{12}$ phase, which discontinuously precipitates along grain boundaries (see Fig. 2(a)). With the increase of Ce content, the grains are refined and the amount and dimension of β phase are reduced. When the Ce content is more than 0.5%, a rod-like intermetallic phase is observed (see the arrows in Figs. 2(d)-(f)). In order to determine the composition of the rod-like intermetallic phase, the comparison between the XRD spectrum of AZ91D alloy and that of AZ91D-0.7% Ce alloy was made (see Fig. 3). The XRD results reveal that the XRD spectrum of AZ91D-0.7% Ce alloy has not only the peaks of $\alpha\text{-Mg}$ matrix and $\beta\text{-Mg}_{17}\text{Al}_{12}$ phase which also appears in that of AZ91D alloy, but also the peak of Al_4Ce phase which doesn't appear in that of AZ91D alloy. Therefore, the rod-like intermetallic phase is determined to be Al_4Ce phase. Because of high thermal stability of Al_4Ce phase, Ce atoms are easily combined with Al atoms to form Al_4Ce phase until all available Ce atoms are consumed without any formation of pseudobinary Mg-Ce or pseudoternary Mg-Al-Ce phases^[11, 14]. During the solidification process, Al_4Ce phase is pushed into the growth interface and the growth of the dendrite is hindered. Therefore, as-cast microstructures of the alloys can be refined. When the Ce content is 0.7%, the refinement effect of the

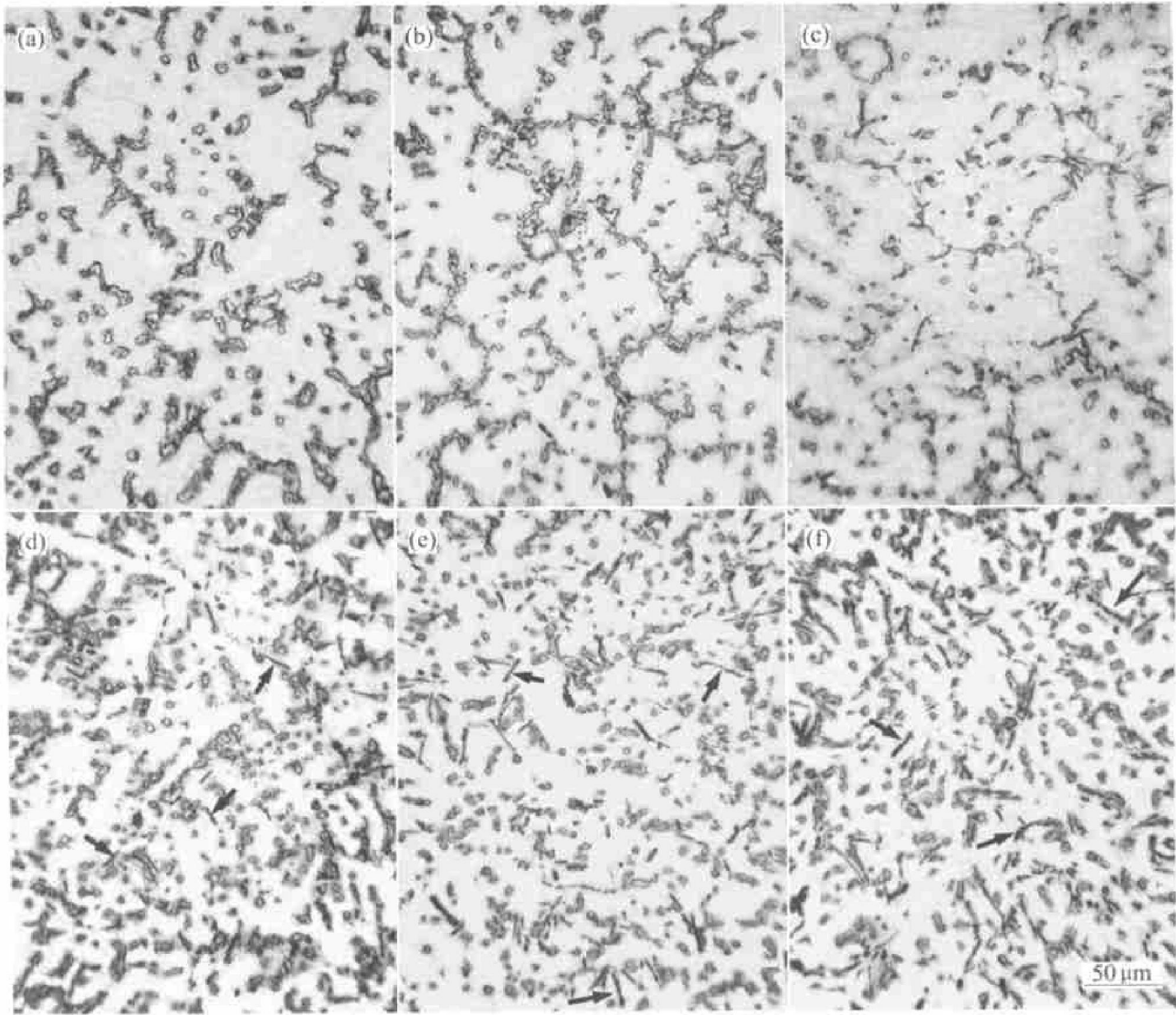


Fig. 2 Microstructures of AZ91D alloys containing various Ce contents
(a) —0% Ce; (b) —0.1% Ce; (c) —0.3% Ce; (d) —0.5% Ce; (e) —0.7% Ce; (f) —1.0% Ce

grains is the most obvious. Meanwhile no reticulate β phase is observed. The amount of Al_4Ce phase reaches the maximum (see Fig. 2(e)). However, the amount of Al_4Ce phase doesn't increase and its size coarsens when the Ce content is over 0.7% (see Fig. 2(f)). Therefore, 0.7% Ce could be a reasonable content to refine the grains of AZ91D alloy.

3.3 Damping mechanism

Fig. 4 shows the plots of damping capacity vs strain amplitude (ϵ) for all specimens. It can be seen that all curves as a whole can be divided into two regions, i.e. strain amplitude independent damping capacity (Q^{-1}) at low strains and strain amplitude dependent damping capacity (Q_H^{-1}) at high strains:

$$Q^{-1} = Q_I^{-1} + Q_H^{-1} \quad (1)$$

The increase of damping capacity with increasing strain amplitude can be explained by the theory of Granato and Lüke^[15, 16], which is based on the breakaway of dislocation segments from weak pinning points. After this breakaway, the segments are

bowled out between weak pinning points which cannot be broken away at low strain amplitude. According to G-L theory, the strain amplitude independent damping capacity (Q_I^{-1}) can be written as

$$Q_I^{-1} = \Lambda b L^4 \omega / (36 G b^2) \quad (2)$$

where Λ is the dislocation density; L is the mean loop length of the weak pinning dislocation segments; ω is the resonant frequency; G is the shear modulus; b is the Burgers vector and B is a parameter.

At high strain amplitude, the dislocation segments break away from the weak pinning points and are free to bow out between the strong pinning points. This leads to an instantaneous increase of strain, and the damping capacity becomes dependent on strain amplitude. According to G-L theory, the strain amplitude dependent damping capacity Q_H^{-1} can be written as

$$Q_H^{-1} = \frac{C_1}{\epsilon} \exp\left(-\frac{C_2}{\epsilon}\right) \quad (3)$$

Here

$$C_1 = \Omega \Lambda_N^3 K \eta_a / (\pi^2 L_C^2) \quad (4)$$

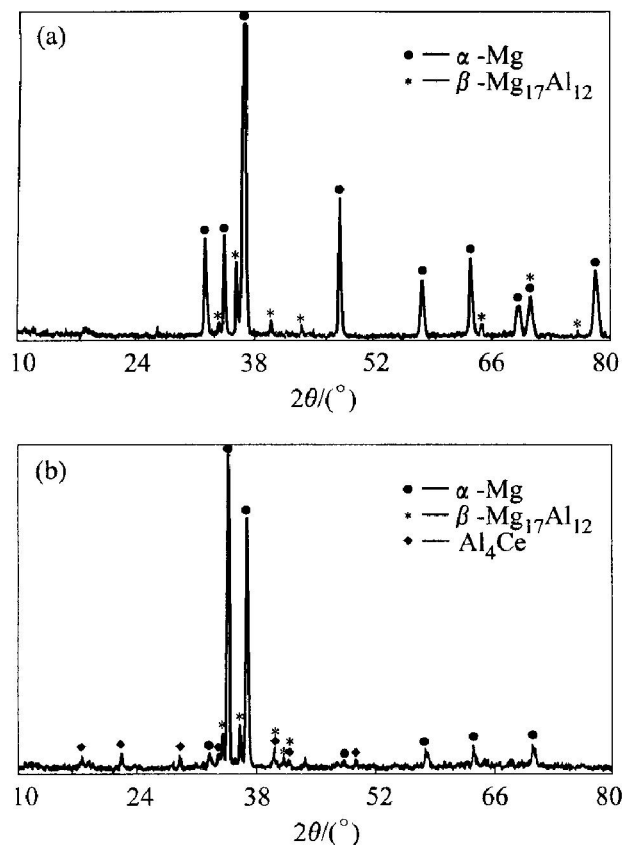


Fig. 3 XRD spectra of AZ91D alloy (a) and AZ91D-0.7% Ce alloy (b)

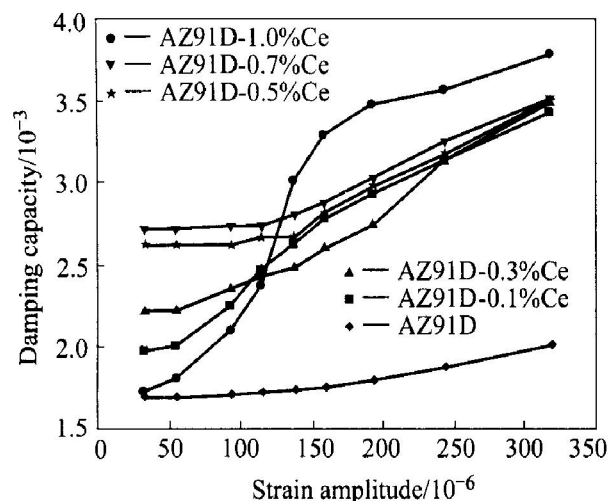


Fig. 4 Strain amplitude dependence of damping capacity of AZ91D alloys containing various Ce contents

$$C_2 = K \Omega a / L_C \quad (5)$$

Where C_1 and C_2 are the physical parameters; ε is the strain amplitude; Ω is the orientation factor; K is a factor depending on the anisotropy of the elastic constants and the orientation of the samples with respect to the applied stress; Ω is the size factor of the pinning solute atoms with respect to the solvent; a is the lattice parameter; L_N and L_C are the length of strong pinning points and weak pinning points respectively.

Then Eqn. (3) can be written as

$$\ln(\varepsilon Q_H^{-1}) = \ln C_1 - \frac{C_2}{\varepsilon} \quad (6)$$

From Eqn. (6), Granato-Lücke (G-L) plots, i. e. $\ln(\varepsilon Q_H^{-1})$ vs ε^{-1} , should be straight lines. Fig. 5 shows the G-L plots for all specimens under high strain amplitude. It can be seen that all G-L plots as a whole exhibit the relationship of straight lines or closing to straight lines. Therefore, the damping behavior of the experimental alloys can be explained by the theory of Granato and Lücke.

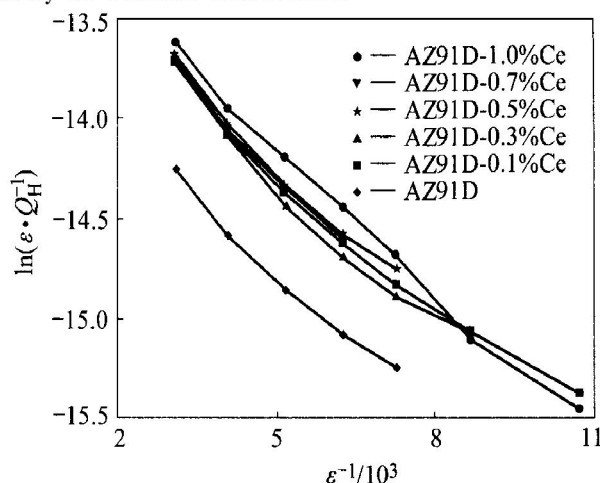


Fig. 5 G-L plots of AZ91D alloys containing various Ce contents

Results shown in Fig. 1 are measured at the strain amplitude of 9.3×10^{-5} , which belongs to low strain amplitude. Therefore, the increasing or reducing trend of the plot can be explained by Eqn. (2). There are mainly two factors to affect the damping capacity, i. e. the dislocation density (Λ) and the mean loop length of the weak pinning dislocation segments (L). β and Al₄Ce phases in the microstructures of AZ91D alloys can be served as strong pinning points. For AZ91D alloys containing small amount of Ce (0.1% Ce and 0.3% Ce), the refinement effect of their microstructures is not obvious compared with unmodified AZ91D alloy. According to the dislocation model, dislocations are thought to be mainly distributed along grain boundaries. Therefore, the amount of dislocations in unit area doesn't increase and the dislocation density (Λ) nearly remains constant. However, the reducing amount and the lessening dimension of β phase can lead to the reduction of strong pinning points. Therefore, both the mean loop length (L) and the damping capacity increases. For AZ91D alloys containing large amount of Ce (0.5% Ce and 0.7% Ce), their microstructures are refined to a large extent, which leads to the increase of the amount of dislocations in unit area. Therefore, dislocation density Λ increases and the damping capacity can be improved. At the same time, the presence and the increase of Al₄Ce phase increase the amount of

strong pinning points, which then reduces the length (L). Therefore, the damping capacity can be reduced. The affecting degree of the former is bigger than that of the latter; therefore the damping capacity continues to increase with the increase of the Ce content. Compared with AZ91D-0.7% Ce alloy, the amount of Al_4Ce phase in the microstructure of AZ91D-1.0% Ce alloy is nearly similar, but their coarsening can reduce the length (L) and lead to the reduction of the damping capacity.

4 CONCLUSIONS

Al_4Ce phase is formed in AZ91D alloy after adding a certain quantity of Ce and as-cast microstructures of the alloys are refined. The refinement effect and damping capacity of the alloys increase with the increase of the Ce content. When the Ce content is 0.7% Ce, the refinement effect is the most obvious and the damping capacity reaches a maximum. Damping capacity (Q^{-1}) of the alloy is 2.728×10^{-3} , 61% increment obtained compared with unmodified AZ91D alloy. The damping capacity of the alloys is relative to strain amplitude, i. e. strain amplitude independence under low strain amplitude and strain amplitude dependence under high strain amplitude. The G-L plots of the alloys under high strain amplitude as a whole exhibit the relationship of straight lines or closing to straight lines. The damping behavior of the alloys can be explained by the theory of Granato and Lücke.

REFERENCES

- [1] Zhang J M, Robert J P, Catherine R W, et al. Effects of secondary phases on the damping behaviour of metals, alloy and metal matrix composites[J]. *Materials Science and Engineering*, 1994, R13(8): 325 - 390.
- [2] Polmear I J. *Magnesium alloys and applications*[J]. *Materials Science and Technology*, 1994, 10(1): 1 - 16.
- [3] Luo A, Pekguleryuz M O. Review cast magnesium alloys for elevated temperature applications[J]. *Journal of Materials Science*, 1994, 29(20): 5259 - 5271.
- [4] Aghion E, Bronfin B. Magnesium alloys development towards the 21st century[J]. *Materials Science Forum*, 2000, 350 - 351(1): 19 - 28.
- [5] Wang Y S, Sun B D, Wang Q D, et al. An understanding of the hot tearing mechanism in AZ91 magnesium alloy[J]. *Materials Letters*, 2002, 53(1): 35 - 39.
- [6] Celotto S. TEM study of continuous precipitation in Mg-9wt% Al-1wt% Zn alloy[J]. *Acta mater*, 2000, 48(8): 1775 - 1787.
- [7] Kageyama H, Shimazu M, Kamado S, et al. Effects of alloying elements and heat treatment on damping capacity of Mg-Al alloys[J]. *Journal of Japan Institute of Light Metals*, 1998, 48(5): 217 - 221.
- [8] Erchov S, Riehemann W, Gabor P, et al. Damping capacity of sand cast magnesium alloy AZ91[J]. *Materials Science and Technology*, 2002, 18(2): 198 - 200.
- [9] Shimizu M, Takeuchi H. Damping capacity of Mg-Al and Mg-Li-Al alloy castings[J]. *International Journal of Cast Metals Research*, 1997, 10(3): 159 - 163.
- [10] LU Yirzhen, WANG Qirong, ZENG Xiaogang, et al. Effects of rare earths on the microstructure, properties and fracture behavior of Mg-Al alloys[J]. *Materials Science and Engineering A*, 2000, 278(1): 66 - 76.
- [11] WANG Qirong, LU Yirzhen, ZENG Xiaogang, et al. Effects of RE on microstructure and properties of AZ91 magnesium alloy[J]. *Trans Nonferrous Met Soc China*, 2000, 10(2): 235 - 239.
- [12] Wei L Y, Dunlop G L. The solidification behaviour of Mg-Al-rare earth alloys[J]. *Journal of Alloys and Compounds*, 1996, 232(3): 264 - 268.
- [13] Wei L Y, Dunlop G L, Westengen H. Development of microstructure in cast Mg-Al-rare earth alloys[J]. *Materials Science and Technology*, 1996, 12(9): 741 - 750.
- [14] ZHANG Shichang, WEI Bokang, LIN Hantong, et al. Effect of yttrium and mischmetal on as-cast structure of AZ91 alloy[J]. *The Chinese Journal of Nonferrous Metals*, 2001, 11(S2): 99 - 102. (in Chinese)
- [15] Granato A, Lücke K. Theory of mechanical damping due to dislocations[J]. *J Appl Phys*, 1956, 27(6): 583 - 593.
- [16] Granato A, Lücke K. Application of dislocation theory to internal friction phenomena at high frequencies[J]. *J Appl Phys*, 1956, 27(7): 789 - 805.

(Edited by LONG Huai-zhong)